Materials Characterization 118 (2016) 411–416

Contents lists available at ScienceDirect

Materials Characterization

journal homepage: www.elsevier.com/locate/matchar

Effect of high pressure torsion on microstructure of Cu-Sn alloys with different content of Hume Rothery phase

A. Korneva [a,*], B. Straumal [b,c,d,e], A. Kilmametov [c], L. Lityńska-Dobrzyńska [a], G. Cios [f], P. Bała [f,g], P. Zięba [a]

[a] Institute of Metallurgy and Materials Science, Polish Academy of Sciences, 25 Reymonta Street, 30-059 Cracow, Poland
[b] Institute of Solid State Physics, Russian Academy of Sciences, Ac. Ossipyan str. 2, 142432 Chernogolovka, Russia
[c] Karlsruhe Institute of Technology (KIT), Institute of Nanotechnology, Hermann-von-Helmholtz-Platz 1, 76344 Eggenstein-Leopoldshafen, Germany
[d] Moscow Institute of Physics and Technology (State University), Institutskii per. 9, 141700 Dolgoprudny, Russia
[e] Laboratory of Hybrid Nanomaterials, National University of Science and Technology "MISIS", Leninskii prosp. 4, 119049 Moscow, Russia
[f] AGH University of Science and Technology, Academic Centre for Materials and Nanotechnology, 30 Mickiewicza Av., 30-059 Crakow, Poland
[g] Faculty of Metals Engineering and Industrial Computer Science, AGH University of Science and Technology, 30 Mickiewicza Av.,30-059 Crakow, Poland

ARTICLE INFO

Article history:
Received 8 April 2016
Received in revised form 16 June 2016
Accepted 16 June 2016
Available online 16 June 2016

Keywords:
Cu–Sn alloys
High-pressure torsion
Microstructure
Hume Rothery phase dissolution
Hardness

ABSTRACT

Two copper alloys with 7.8 and 23 at.% tin with different content of ε Hume Rothery phase were subjected to high pressure torsion (HPT) at room temperature. The initial state of both alloys before HPT was quite different. The first alloy contained the Cu matrix (α-phase) with uniformly distributed precipitates of ε-phase, while another consisted of alternating plates of the ε phase and fine-grained (α + ε) mixture. Strong grain refinement of α phase to the nanometer range and partial dissolution of ε phase in Cu-matrix were observed in the Cu–7.8 at.% Sn alloy after HPT. The Cu–23 at.% Sn alloy after HPT revealed neither the grain refinement nor dissolution of phases.

1. Introduction

The severe plastic deformation (SPD) can induce strong grain refinement of microstructure and frequently leads to various phase transformations like the formation [1,2] or decomposition of a supersaturated solid solution [3,4], dissolution of phases [5,6], amorphization of crystalline phases [7,8], the decomposition of an amorphous phase with the formation of nanocrystals [9,10] or allotropic phase transformation [11,12]. However, those phase transformations were usually observed in the phases with a relatively simple crystal lattice such as fcc, bcc or hcp structures. The examples of such phase transformations can be α → ω phase transition in Ti after high pressure torsion (HPT) [11], the β → ω transition in metastable Ti–V alloys after hot rolling [12] or the decomposition of supersaturated solid solution in systems Al-Zn, Co-Cu, Cu-Ni after HPT [4]. It should be noted, that the systems of last examples are characterized by positive mixing enthalpy and do not contain any intermetallic compounds. There are also many works dedicated to grain refinement and property changes of intermetallic phases (such as TiAl [13], Fe_3Al [14,15], TiNi and Ni_3Al [15], Zr_3Al [16]) with more complex crystal structures analyzed after SPD. However, the phase transformations of intermetallic phases induced by SPD, especially in the Cu-Sn alloys, are not as much referred to in the literature. The Cu-Sn system is characterized by negative mixing enthalpy and different combinations of intermetallic Hume Rothery phases (or electron compounds), such as δ ($Cu_{41}Sn_{11}$) phase with cubic crystal lattice, ε (Cu_3Sn) phase with orthorhombic crystal lattice or ζ ($Cu_{10}Sn_3$) phase with hexagonal crystal lattice. Hume Rothery phases are the phases, in which a small change in the concentration can lead to a strong change in the crystal lattice [17,18]. The examination of SPD effect on the microstructure evolution and hardness of the Cu-23 at.% Sn alloy in (ζ + ε) state was studded in the previous work [19]. The aim of this work was to study the influence of SPD on microstructure and possible phase transformations in two copper alloys with 7.8 and 23 at.% tin in the (α + ε) state with different amounts of intermetallic ε Hume Rothery phase.

2. Experimental procedure

Two copper alloys with 7.8 and 23 at.% tin were manufactured by induction melting in vacuum. The resulting ingots with the diameter of 10 mm were cut into 0.7 mm thick disks. These disks were homogenized at the temperature of 320 °C for a long time (1200 h). This temperature corresponds to the two-phase state (copper based solid solution and ε phase) according to the Cu–Sn equilibrium phase diagram [20]. After the homogenization the samples were quenched in

* Corresponding author.
E-mail address: a.korniewa@imim.pl (A. Korneva).

http://dx.doi.org/10.1016/j.matchar.2016.06.019
1044-5803/

water in order to preserve the chemical composition of the α-matrix (up to 6 wt.% of Sn). In that way the influence of SPD on the ε phase behavior in dependence on its volume fraction at the same solubility of Sn in the Cu-matrix could be examined. Afterwards, the disks were subjected to high pressure torsion (HPT) in a Bridgman anvil chamber (W. Klement GmbH, Lang, Austria) at the pressure of 7 GPa and five revolutions at speed 1 rpm at room temperature. The samples for the microstructure studies were cut off at the distance of 3 mm from the center of the deformed disk. For the metallographic investigations the samples were ground with SiC paper, followed by polishing with 6, 3 and 1 μm diamond pastes. The prior inspection of the obtained material was carried out on a Philips XL30 scanning electron microscope (SEM) equipped with a LINK ISIS an energy-dispersive X-ray spectrometer (EDS) produced by Oxford Instruments. The nanoscale details of the phases were revealed using a TECNAI G2 FEG super TWIN (200 kV) transmission electron microscope (TEM) equipped with an energy dispersive X-ray (EDX) spectrometer manufactured by EDAX. Calibration of the EDX measurements was made by checking positions of the Kα lines of Co and Al. The quantitative results of EDX were calculated by the software TEM Imaging and Analysis (TIA), FEI Company. Thin foils of the Cu–7.8 at.% Sn alloy for TEM observation were prepared by a twin-jet polishing technique using the mixture of 33 vol.% nitric acid and 67 vol.% methanol cooled to − 30 °C. The Cu–23 at.% Sn alloy proved to be very brittle and the focused ion beam (FIB) technique by means of FIB Quanta 3 D, TECNAI FEG microscopy (30 kV) was applied for the preparation of thin foils. X-ray diffraction patterns were obtained in the Bragg–Brentano geometry on a Philips X'Pert powder diffractometer with the use of Cu-*K*α radiation. The lattice parameter was determined by means of the Fityk program using Rietveld approach for full-profile analysis [21]. The phases in the alloys were identified according to the X'Pert HighScore PANalytical phase database [22]. The hardness was measured using an AGILENT G200 nanoindenter with XP head at the load of 10 mN.

3. Results and discussion

The microstructure observation of the Cu–7.8 at.% Sn alloy after homogenization at 320 °C by the backscatter electron mode in SEM showed the presence of mixture of (α + ε) phases, which was uniformly distributed in the Cu matrix (Fig. 1a). The mixture was enriched with tin up to 16 at.%. The chemical composition of the Cu matrix was inhomogeneous: the amount of tin in the matrix changed from about 2 to 5 at.% (Table 1), which corresponds to a different contrast (from dark to gray color) of the matrix, obtained in the BSE/SEM mode and visible in Fig. 1a. The X-ray diffraction patterns (Fig. 2a) showed peaks from α and ε phases. The α phase (or (Cu)) is a copper-based solid solution with the fcc structure, the space group *Fm3m*, and the lattice constant $a = 3.6605 \pm 0.0001$ Å. This parameter was larger than that in pure copper (3.6157 Å [23]) due to the tin dissolved in the α-matrix. The ε phase (or Cu_3Sn) has an orthorhombic structure with the space group *Cmcm* [24] and lattice constants $a = 5.5132 \pm 0.0001$ Å, $b = 38.9567 \pm 0.0001$ Å, and $c = 4.3882 \pm 0.0001$ Å. TEM investigations confirmed that the microstructure contained the α-matrix and the mixture of the fine-grained α and ε phases (Fig. 1b).

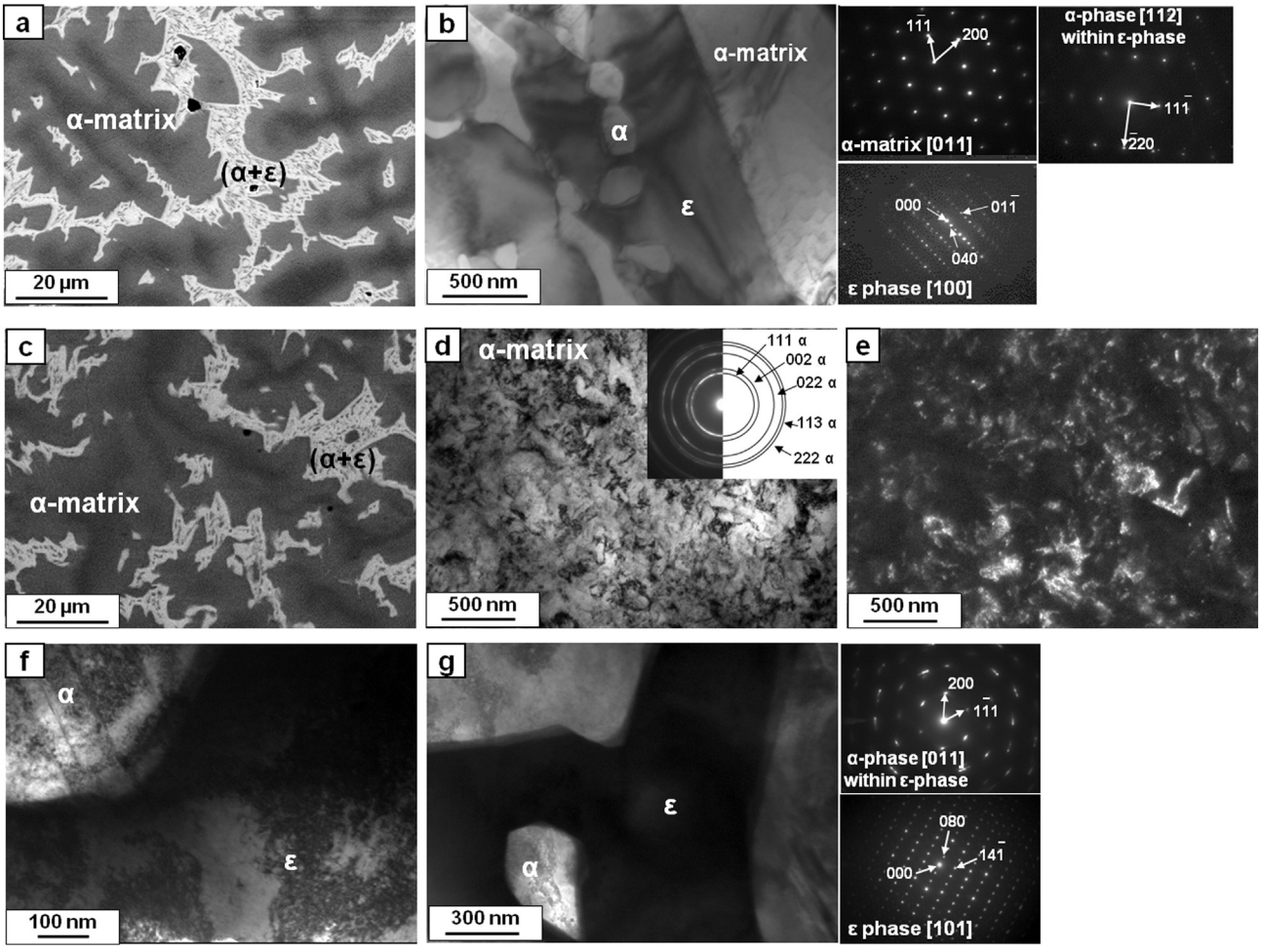

Fig. 1. SEM (a, c) and TEM (b, d–g) micrographs with SAED patterns of the Cu–7.8 at.% Sn alloy after homogenization at 320 °C for 1200 h (a, b) and after HPT (c–g). Bright field (d) and dark field (e) images of the deformed α-matrix. Bright field images of the deformed (α + ε) mixture (f, g).

Table 1
The chemical composition of phases before and after HPT process of the Cu-7.8 at.% Sn alloy, at.%, EDS/SEM.

Phase	Before HPT		After HPT	
	Cu	Sn	Cu	Sn
α-matrix with a dark color in Fig. 1a, c	97.8 ± 1.9	2.2 ± 0.1	97.0 ± 1.9	3.0 ± 0.1
α-matrix with a gray color in Fig. 1a, c	95.1 ± 1.9	4.9 ± 0.2	94.3 ± 1.9	5.7 ± 0.2
(α + ε) mixture	83.9 ± 1.7	16.1 ± 0.3	84.4 ± 1.7	15.6 ± 0.3

Table 2
The hardness of phases in the Cu-7.8 at.% Sn and Cu-23 at.% Sn alloys before and after HPT process, GPa.

Alloy	Phases	Before HPT	After HPT
Cu-7.8 at.% Sn	α	1.8 ± 0.2	3.5 ± 0.3
	(α + ε)	5.0 ± 0.6	5.6 ± 0.6
Cu-23 at.% Sn	ε	6.3 ± 0.4	6.6 ± 0.5
	(α + ε)	5.4 ± 0.7	6.3 ± 0.9

The SEM microstructure of the Cu–7.8 at.% Sn alloy after HPT is presented in Fig. 1c. It appears, that the mixture of α and ε phases was preserved and remained surrounded by the α-matrix. The measurements of chemical composition by EDS/SEM after HPT showed that tin content in the (α + ε) mixture slightly decreased and tin content in the matrix rose a little (Table 1). Thus, the partial dissolution of tin from the ε phase occurred.

The broadening of the XRD peaks from the α phase observed after deformation (Fig. 2b), indicated strong grain refinement (common for HPT) and significant microdistortions of the crystal lattice. The TEM micrographs confirmed the strong grain refinement of the α-matrix (the grain sizes changed from about 300 to 50 nm) visible as diffraction rings in the selected area electron diffraction pattern (obtained from the area about 12 μm^2) (upper corner in Fig. 1d) and corresponding dark field image (Fig. 1e). A slight shift of the copper XRD peaks to lower diffraction angles was additionally observed. This corresponds with the increase of lattice parameters of Cu-matrix up to 3.6748 Å, resulting from the partial dissolution of tin atoms from the ε phase in the matrix. The XRD peaks from the ε phase became blurred and almost invisible, which may indicate that the mixture (α + ε) could be refined also through deformation. However, the TEM observation of the mixture did not show its refinement after HPT, apart from a strong increase of dislocation density within the grains of the (α + ε) mixture (Fig. 1f, g).

In order to understand why the mixture of α and ε phases did not show grain refinement after HPT, the measurements of microhardness were performed. It turned out that the fine mixture of α and ε phases was harder in comparison with the α-matrix. Its hardness was about three times higher than that of the matrix before deformation. The hardness of the deformed Cu matrix increased by about 94% (from 1.8 ± 0.2 to 3.5 ± 0.3 GPa) probably mainly due to grain refinement, while hardness of the mixture increased only by 12% (from 5.0 ± 0.6 to 5.6 ± 0.6 GPa) (Table 2) presumably as result of the increase of dislocation density and amount of stacking faults in the deformed α grains of the (α + ε) mixture. Therefore, it is possible that the mixture did not show grain refinement after deformation due to its high hardness. The similar behavior of two-phase material containing the hard second phase in the soft matrix subjected to HPT deformation was observed in the Cu-22 wt.% In alloy [25]. The hardness of intermetallic δ (Cu_7In_3) phase before deformation reached 2 GPa, while the hardness of Cu-based solid solution (α phase) was only 1 GPa [21]. After deformation the strong grain refinement of the matrix was observed, while the δ phase appeared intact, i.e. neither dissolved nor refined. This unusual behavior of the δ phase was related to its significant hardness. On the other hand, it should be noted that hard particles in the soft matrix do not always retain their shape after plastic strain. For example, Cu–Fe alloy contained soft Cu matrix and hard α-Fe particles (the difference in hardness was about two times). Nevertheless, the refinement of iron particles during SPD has been observed [26,27].

The microstructure of the alloy with 23 at.% Sn alloy after homogenization at 320 °C was strongly different from the alloy with 7.8 at.% Sn after the same heat treatment. The microstructure consisted of alternating plates of the ε phase and a mixture of the (α + ε) phases with the thickness of about 60 and 120 μm, respectively (Fig. 3a, b). Some plates of the ε phase revealed irregular morphology with characteristic grooves indicated with arrows in Fig. 3a, d. The microstructure

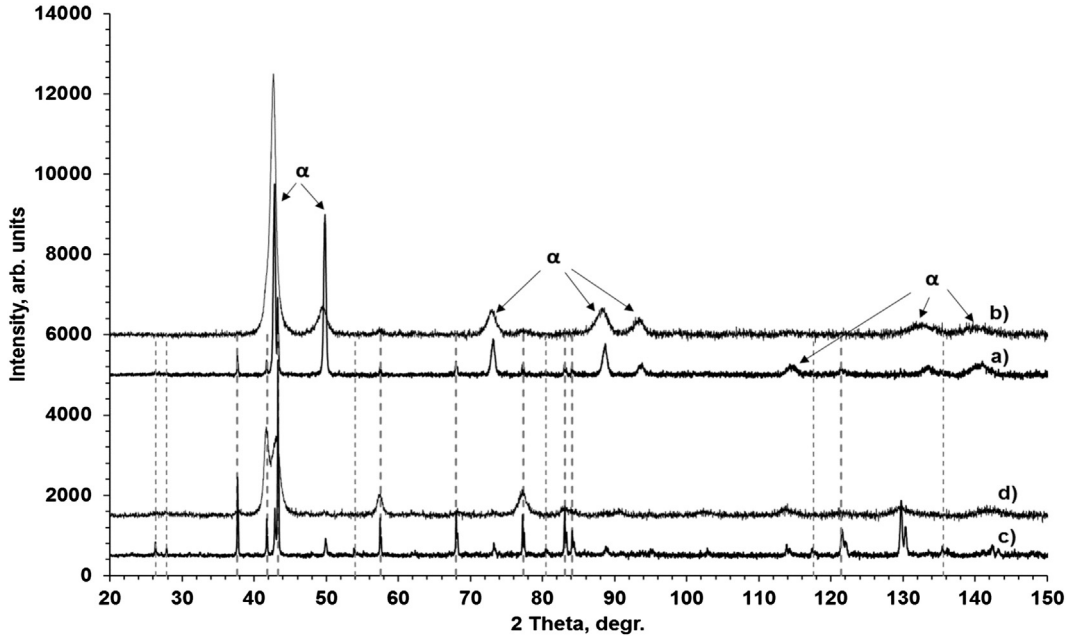

Fig. 2. X-ray diffraction patterns of the Cu–7.8 at.% Sn (a, b) and Cu–23 at.% Sn (c, d) alloys after homogenization at 320 °C for 1200 h (a, c) and after HPT (b, d). The vertical dashed lines indicate the angular positions of 2 theta angles for the ε phase.

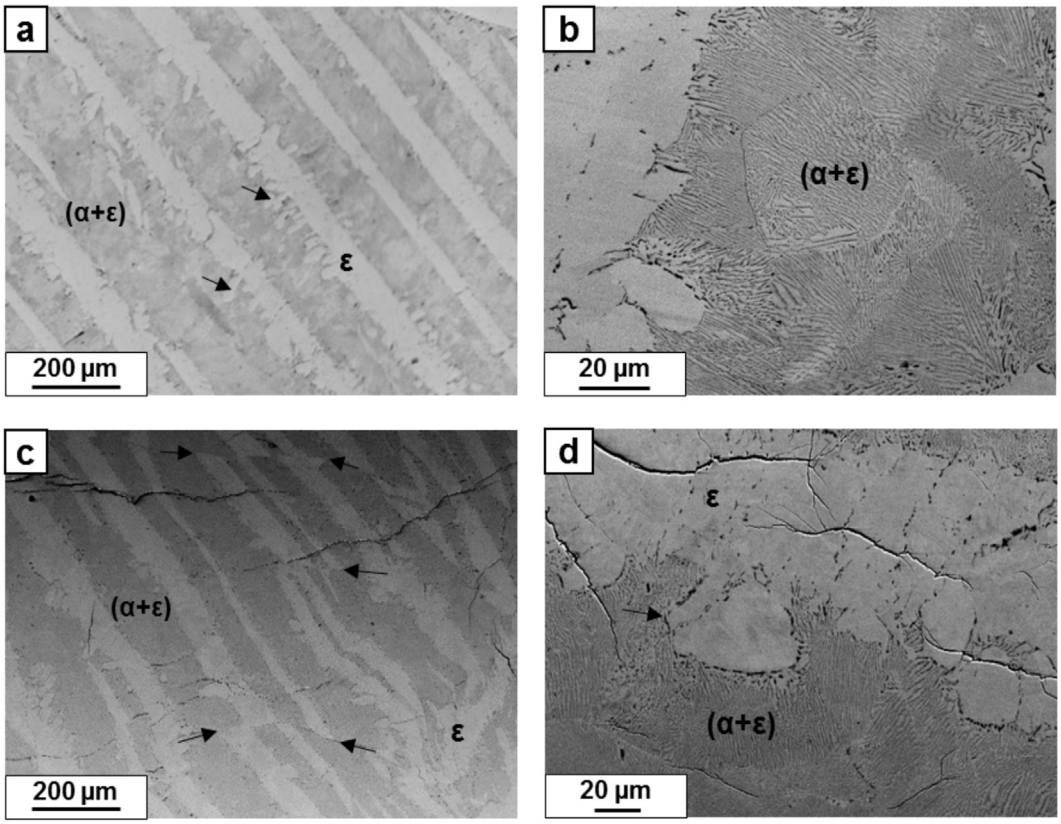

Fig. 3. SEM micrographs of the Cu–23 at.% Sn alloy after homogenization at 320 °C for 1200 h (a, b) and after homogenization at 320 °C for 1200 h and HPT (c, d). Arrows in Figs. a and d indicate irregular morphology of ε plates with characteristic grooves. Arrows in Fig. c indicate the shear lines in the ε plates after HPT.

observation after HPT showed a high number of large and small cracks on the surface of deformed sample (small cracks especially located inside the brittle ε phase). Generally, the plates of the ε phase after HPT were preserved, although some plates were intersected by cracks (arrows in Fig. 3c) or slightly curved. The thickness of the plates of the ε phase and mixture (α + ε) remained almost the same. The tin content measured by EDS/SEM in the ε phase and in the mixture of (α + ε) phases did not change after HPT and was about 23.6 ± 0.9 and 21.0 ± 0.8 at.%, respectively. The X-ray patterns of the Cu–23 at.% Sn alloy before and after HPT are presented in Fig. 2c, d, respectively. The intensity of α peaks before HPT is very low in comparison with the alloy containing 7.8 at.% Sn, because according to the lever rule applied to the equilibrium Cu–Sn phase diagram, the volume fraction of α phase is about 6%, while in the Cu–7.8 at.% alloy it reaches about 80%. The lattice parameter of the α-phase before HPT was 3.6522 Å. Unfortunately, the measurement of lattice parameter for the α-phase after HPT could not be performed, because at least 5 peaks have to be taken into account for a reliable analysis of the lattice parameters. Unfortunately, after HPT only one peak (111) of the α phase was visible since the fcc phase after severe plastic deformation usually has a tendency to form a crystallographic texture [28,29]. Additionally, the (111) peak overlapped with the (002) peak of the ε-phase. Intensity of other peaks significantly decreased and became almost equal to the level of background.

The TEM observation of the Cu–23 at.% Sn alloy after HPT revealed that the α grains (Fig. 4a) were elongated with the transverse size about 120 nm. The tin content (measured by EDX/TEM) in the deformed α grains was about 4.5 ± 0.2 at.%. The α and ε phases in the mixture are

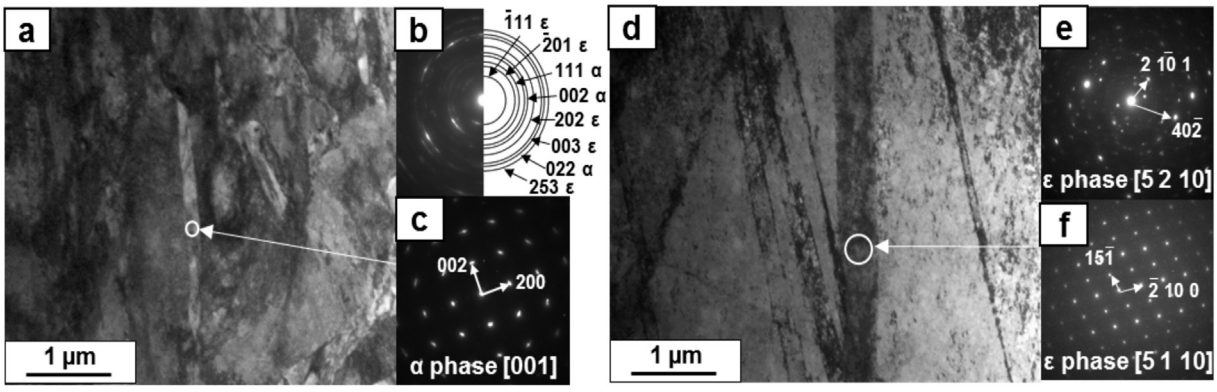

Fig. 4. TEM micrographs (a) of the (α + ε) mixture and (d) of the ε plate of the Cu–23 at.% Sn alloy after homogenization at 320 °C for 1200 h and followed by HPT with SAED patterns (b, c, e, f). The SAED patterns (b, e) were obtained from the whole visible area in Figs. a and d, while the SAED patterns (c, f) were obtained from the separated α and ε grains (marked by rings) in Figs. a and d. Reflections (2 − 101) and (4 0–2) for orientation [5 2 10] of ε phase were determined in Fig. e, but it should be noted, that this diffraction pattern contains also some reflections from other orientations of ε phase.

characterized by a high density of dislocations. The electron diffraction of the mixture obtained from the area about 12 μm^2 showed discontinuous rings and some elongated spots (Fig. 4b). The discontinuous rings show an initial state of microstructure refinement and are likely associated with the existence of small amount of grains. The elongated spots are attributed to a high density of dislocation and stacking faults. The high density of dislocation was observed within the plates of the ε phase also and the formation of plate-like microstructure with different contrast bands running across the bright field in various directions was visible (Fig. 4d). Thin plates of different thickness from about 40 to 400 μm were observed. The corresponding electron diffraction obtained from the area 12 μm^2 showed a small number of diffraction spots (Fig. 4e).

The measurements of hardness showed the increase of hardness from 6.3 ± 0.4 to 6.6 ± 0.5 GPa for the plates of ε phase and from 5.4 ± 0.7 to 6.3 ± 0.9 GPa for the mixture of (α + ε) phases (Table 2). Such a slight increase of hardness may be associated with a high density of dislocation induced by HPT process. It should be noted, that hardness measurement did not result in the appearance of additional new cracks in the both phases.

The HPT usually induces strong grain refinement and phase transformations. For example, the HPT resulted in a partial dissolution of the Co particles in the Cu–4.9 wt.% Co [23] alloy or decomposition of supersaturated solid solution in the Cu–77 wt.% Ni alloy [5]. However, in the case of Cu–23 at.% Sn alloy, only a slight bending or sometimes a shift of one part relative to the other part of the ε plates in cross-section were observed. Neither grain refinement nor dissolution of phases were noticed. It seems that unusual behavior of the alloy was connected with the large volume fraction of very hard ε phase of a complicated orthorhombic crystal lattice (20 atoms per cell unit). It should be noted that the hardness of ε phase was close to the hardness of the surrounding plates belonging to the mixture of the (α + ε) phases. In the case of the Cu–7.8 at.% Sn alloy a partial dissolution of the ε phase was possible due to a low volume fraction of this phase which was surrounded by the soft α-matrix. The similar situation of the partial dissolution of the intermetallic hard δ (Cu_7In_3) phase contained in the soft α-matrix in the Cu–22 wt.% In alloy after HPT was observed also in Ref. [30] where the volume fraction of δ phase reached about 20%. This quick dissolution takes place despite of the fact that the applied pressure of 7 GPa slows down the diffusion as well as grain boundary migration [31, 32].

4. Conclusions

The homogenization at 320 °C of the Cu–7.8 at.% Sn alloy resulted in the formation of the mixture of (α + ε) phases in the Cu matrix. After HPT the strong grain refinement of Cu-matrix and the partial dissolution of the ε phase were observed. The increase of tin content up to 23 at.% and homogenization at 320 °C was the reason for the appearance of microstructure strongly different from that observed in the alloy with 7.8 at.% tin. Thick alternating plates of the ε phase and the mixture of the (α + ε) phases were observed with the overall volume fraction of ε phase about 94%. The microstructure observations of deformed alloy showed an unexpected phenomenon: neither grain refinement nor the dissolution of phases were noticed. Most likely, the unusual behavior of the Cu–23 at.% Sn alloy was connected with the large volume fraction of very hard ε-phase with a complicated orthorhombic crystal lattice.

The research has been performed within the Accredited Testing Laboratories with certificate No. AB 120 issued by the Polish Centre of Accreditation according to European standard PN-ISO/IEC 17025:2005 and EA-2/15.

The work was supported by the National Science Centre of Poland (grant OPUS 2014/13/B/ST8/04247), the Russian Federal Ministry for Education and Science (grants 14.A12.31.0001 and Increase Competitiveness Program of NUST "MISiS") and by the Russian Foundation for Basic Research (grant 15-08-09325).

References

[1] W. Lojkowski, M. Djahanbakhsh, G. Burkle, S. Gierlotka, W. Zielinski, H.J. Fecht, Nanostructure formation on the surface of railway tracks, Mater Sci Eng A 303 (2001) 197–208, http://dx.doi.org/10.1016/S0921-5093(00)01947-X.
[2] V.V. Stolyarov, R. Lapovok, I.G. Brodova, P.F. Thomson, Ultrafine-grained Al–5 wt.% Fe alloy processed by ECAP with backpressure, Mater Sci Eng A 357 (2003) 159–167, http://dx.doi.org/10.1016/S0921-5093(03)00215-6.
[3] B.B. Straumal, B. Baretzky, A.A. Mazilkin, F. Phillipp, O.A. Kogtenkova, M.N. Volkov, R.Z. Valiev, Formation of nanograined structure and decomposition of supersaturated solid solution during high pressure torsion of Al–Zn and Al–Mg alloys, Acta Mater 52 (2004) 4469–4478, http://dx.doi.org/10.1016/j.actamat.2004.06.006.
[4] B. Straumal, A. Korneva, P. Zięba, Phase transitions in metallic alloys driven by the high pressure torsion, Arch. Civ. Mech. Eng. 14 (2014) 242–249, http://dx.doi.org/10.1016/j.acme.2013.07.002.
[5] Y. Ivanisenko, W. Lojkowski, R.Z. Valiev, H.J. Fecht, The mechanism of formation of nanostructure and dissolution of cementite in a pearlitic steel during high pressure torsion, Acta Mater 51 (2003) 5555–5570, http://dx.doi.org/10.1016/S1359-6454(03)00419-1.
[6] S. Ohsaki, S. Kato, N. Tsuji, T. Ohkubo, K. Hono, Bulk mechanical alloying of Cu–Ag and Cu/Zr two-phase microstructures by accumulative roll-bonding process, Acta Mater 55 (2007) 2885–2895, http://dx.doi.org/10.1016/j.actamat.2006.12.027.
[7] A.A. Mazilkin, G.E. Abrosimova, S.G. Protasova, B.B. Straumal, G. Schütz, S.V. Dobatkin, A.S. Bakai, Transmission electron microscopy investigation of boundaries between amorphous "grains" in Ni50Nb20Y30 alloy, J Mater Sci 46 (2011) 4336–4342 (doi: 10.1007/s10853-011-5304-3).
[8] A.V. Sergueeva, C. Song, R.Z. Valiev, A.K. Mukherjee, Structure and properties of amorphous and nanocrystalline NiTi prepared by severe plastic deformation and annealing, Mater Sci Eng A 339 (2003) 159–165, http://dx.doi.org/10.1016/S0921-5093(02)00122-3.
[9] A.M. Glezer, M.R. Plotnikova, A.V. Shalimova, S.V. Dobatkin, Severe plastic deformation of amorphous alloys: I. Structure and mechanical properties, Bull. Russ. Ac. Sci. Phys. 73 (2009) 1233–1239.
[10] G.E. Abrosimova, A.S. Aronin, S.V. Dobatkin, S.D. Kaloshkin, D.V. Matveev, O.G. Rybchenko, E.V. Tatyanin, I.I. Zverkova, The formation of nanocrystalline structure in amorphous Fe-Si-B alloy by severe plastic deformation, J. Metastable Nanocryst. Mater. 24 (2005) 69–72 (doi: s10.4028/www.scientific.net/JMNM.24-25.69).
[11] Y. Ivanisenko, I. MacLaren, X. Sauvage, R.Z. Valiev, H.-J. Fecht, Shear-induced α → γ transformation in nanoscale Fe–C composite, Acta Mater 54 (2006) 1659–1669, http://dx.doi.org/10.1016/j.actamat.2005.11.034.
[12] X.L. Wang, L. Li, W. Mei, W.L. Wang, J. Sun, Dependence of stress-induced omega transition and mechanical twinning on phase stability in metastable β Ti–V alloys, Mater Charact 107 (2015) 149–155, http://dx.doi.org/10.1016/j.matchar.2015.06.038.
[13] S.M.L. Sastry, R.N. Mahapatra, Grain refinement of intermetallics by severe plastic deformation, Mater Sci Eng A 329–331 (2002) 872–877, http://dx.doi.org/10.1016/S0921-5093(01)01644-6.
[14] D.G. Morris, M.A. Muñoz-Morris, Microstructural refinement in alloys and intermetallics by severe plastic deformation, J Alloys Compd 536 (2012) 180–185, http://dx.doi.org/10.1016/j.jallcom.2011.10.069.
[15] R.Z. Valiev, A.K. Mukherjee, Nanostructures and unique properties in intermetallics, subjected to severe plastic deformation, Scr Mater 44 (2001) 1747–1750, http://dx.doi.org/10.1016/S1359-6462(01)00795-3.
[16] D. Geist, C. Gammer, C. Mangler, C. Rentenberger, H.P. Karnthaler, Electron microscopy of severely deformed $L1_2$ intermetallics, Philos. Mag. 90 (2010) 4635–4645, http://dx.doi.org/10.1080/14786435.2010.482178.
[17] T.B. Massalski, U. Mizutani, Electronic structure of Hume-Rothery phases, Prog. Mater. Sci. 22 (1978) 151–262, http://dx.doi.org/10.1016/0079-6425(78)90001-4.
[18] Y.S. Umanskii, Y.A. Skakov, Physics of Metals (Atomic Structure of Metals and Alloys), Metallurgiya, Moscow, 1978 (in Russian).
[19] A. Korneva, B. Straumal, R. Chulist, A. Kilmametov, P. Bała, G. Cios, N. Schell, P. Zięba, Grain refinement of intermetallic compounds in the Cu-Sn system under high pressure torsion, Mater Lett 179 (2016) 12–15, http://dx.doi.org/10.1016/j.matlet.2016.05.059.
[20] S. Fürtauer, D. Li, D. Cupid, H. Flandorfer, The Cu–Sn phase diagram, part I: new experimental results, Intermetallics 34 (2013) 142–147, http://dx.doi.org/10.1016/j.intermet.2012. 10.004.
[21] M. Wojdyr, Fityk: a general-purpose peak fitting program, J. Appl. Crystallogr. 43 (2010) 1126–1128.
[22] D. Smith, et al., ICDD Grant_in_Aid, Penn State Univ, Univ. Park, Pennsylvania, 1978.
[23] B.B. Straumal, A.R. Kilmametov, Y.O. Kucheev, L. Kurmanaeva, Y. Ivanisenko, B. Baretzky, A. Korneva, P. Zięba, D.A. Molodov, Phase transitions during high pressure torsion of Cu–Co alloys, Mater Lett 118 (2014) 111–114, http://dx.doi.org/10.1016/j.matlet. 2013.12.042.
[24] Y. Watanabe, Y. Fujinaga, H. Iwasaki, Lattice modulation in the long-period superstructure of Cu_3Sn, Acta Crystallogr B 39 (1983) 306–311, http://dx.doi.org/10.1107/S010876 8183002451.
[25] A. Korneva, B. Straumal, O. Kogtenkova, Y. Ivanisenko, A. Wierzbicka-Miernik, A. Kilmametov, P. Zieba, Microstructure evolution of Cu – 22% in alloy subjected to the high pressure torsion, IOP Conf. Ser. Mater. Sci. Eng. 63 (2014) 012093, http://dx.doi.org/10.1088/1757-899X/63/1/012093.
[26] N.D. Stepanov, A.V. Kuznetsov, G.A. Salishchev, N.E. Khlebova, V.I. Pantsyrny, Evolution of microstructure and mechanical properties in Cu–14%Fe alloy during severe cold rolling, Mater Sci Eng A 564 (2013) 264–272, http://dx.doi.org/10.1016/j.msea.2012.11.121.

[27] N.D. Stepanov, A.N. Kozin, G.A. Salishchev, N.E. Khlebova, V.I. Pantsyrny, Effect of ECAP on microstructure and mechanical properties of Cu-14Fe microcomposite alloy, IOP Conf. Ser.: Mater. Sci. Eng. 63 (2014) 012098, http://dx.doi.org/10.1088/1757-899X/63/1/012098.
[28] I.V. Alexandrov, K. Zhang, A.R. Kilmametov, K. Lu, R.Z. Valiev, The X-ray characterization of the ultrafine-grained Cu processed by different methods of severe plastic deformation, Mater Sci Eng A 234–236 (1997) 331–334.
[29] I.V. Alexandrov, A.A. Dubravina, A.R. Kilmametov, V.U. Kazykhanov, R.Z. Valiev, Textures in nanostructured metals processed by severe plastic deformation, Met. Mater. Int. 9 (2003) 151–156.
[30] B.B. Straumal, A.R. Kilmametov, A.A. Mazilkin, L. Kurmanaeva, Y. Ivanisenko, A. Korneva, P. Zięba, B. Baretzky, Transformations of Cu(in) supersaturated solid solutions under high-pressure torsion, Mater Lett 138 (2015) 255–258, http://dx.doi.org/10.1016/j.matlet.2014.10.009.
[31] B.B. Straumal, L.M. Klinger, L.S. Shvindlerman, The influence of pressure on indium diffusion along single tin-germanium interphase boundaries, Scr. Metall. 17 (1983) 275–279, http://dx.doi.org/10.1016/0036-9748(83)90156-4.
[32] D.A. Molodov, B.B. Straumal, L.S. Shvindlerman, The effect of pressure on migration of 001 tilt grain boundaries in tin bicrystals, Scripta Metall. 18 (1984) 207–211, http://dx.doi.org/10.1016/0036-9748(84)90509-X.